

Computational Fluid Dynamics (CFD) Analysis and Experimental Study for Toxic Hazardous Waste Destruction in the Cavity Incinerator

Young Nam Chun[†]

Department of Environmental Engineering, Chosun University, 375 Seosuk-dong, Dong-gu, Gwangju 501-759, Korea
(Received 20 October 2002 • accepted 28 February 2003)

Abstract—We undertook numerical and experimental studies to develop a better incineration method for the destruction of CCl_4 . A phenomenological model for the turbulent reaction of CCl_4 , including a flame inhibition feature, has been successfully incorporated into a commercial code, simulating the incineration processes of this compound. The gaseous flow solution was obtained using SIMPLEST, a derivative of Patankar's SIMPLE algorithm, with a $k-\epsilon$ turbulence model. A modified fast chemistry turbulent reaction model was developed to describe the flame inhibition due to the presence of CCl_4 , considering the corresponding burning velocity data of these mixtures. An experiment was carried out on a 5.2 kW laboratory scale, transportable, cavity-type incinerator, which warrants a sufficient residence time and effective turbulent mixing by the formation of a strong recirculation region in a combustor. To this end, the specific configuration of the incinerator was manufactured to consist of two opposing jets and a rearward facing step. The calculated data were in close agreement with the experimental data for the concentrations of major species, such as CCl_4 and HCl , together with the temperature profiles. The experimental test gave the desired DRE of above 99.99%.

Key words: Hazardous Waste, Cavity Incinerator, Reaction Model, CCl_4 , Flame Inhibition

INTRODUCTION

Incineration is an attractive alternative for the treatment of several classes of toxic hazardous wastes. Particularly, a cavity-type incinerator, located on the same site where the waste is generated usually, has been considered as an attractive incinerator for less opposition from the public. A cavity incinerator is generally characterized by the sudden expansion of a fuel-air mixture into a combustion cavity formed by a rearward facing step. This gives higher residence time in the recirculation zone. Therefore, it has a long enough reaction time for hazardous waste to be destroyed at high temperature.

Models of industrial boilers have been developed to predict the combustion process performance [McKenty et al., 1999]. However, these studies have made use of simplifying assumptions and do not provide detailed distribution of the turbulent flow fields, temperature and species concentrations in a combustor. In addition, analytical studies of the combustion dynamics in the cavity incinerator have recently been carried out [Liou et al., 2001; Stone and Menon, 2001]. However, a phenomenological model for the turbulent reaction of CCl_4 , including flame inhibition feature, has not been studied with CFD (computational fluid dynamics) analysis, which would simulate the incineration processes of CCl_4 . Most past studies have focused on flame stability and DRE (destruction and removal efficiency) [Gutmark et al., 1996; Cole et al., 2001], but did not utilize the large hot recirculation zone in the combustion cavity, as in oxidizing chemical reactors, for the destruction of hazardous wastes. Use of the combustion cavity in the cavity incinerator, for greater destruction of hazardous waste, requires the development of a compact incinerator.

In this study, a phenomenological model for the turbulent reaction of CCl_4 , including a flame inhibition feature, has been incorporated into a commercial code (PHOENICS Version 3.3) to simulate the incineration processes of this compound. We proposed an advanced cavity incinerator having a combustion cavity, as in an oxidizing chemical reactor, while a steady three-dimensional model, constructed for this study, was used to find the characteristics of the flame structure, combustion cavity and CCl_4 destruction. Systematic parametric studies were made in order to obtain useful information for optimum design, and operating conditions. Further experimental tests, in the 5.2 kW laboratory scale incinerator, were carried out to use in these comparisons and to demonstrate the attainment of the desired DRE, of above 99.99%, before being applied to a full-scale plant.

EXPERIMENTAL APPARATUS AND PROCEDURE

The experimental apparatus used in the present study is shown in Fig. 1, as well as details of the dump incinerator.

The 5.2 kW insulated, castable, laboratory scale incinerator was constructed to use in these comparisons and to show the attainment of the desired DRE, before application to a full-scale plant. It was designed for making detailed measurements in the combustion cavity, having 16 sampling ports.

Fuel (CH_4) and air were mixed and introduced into the auxiliary burner and waste injector, respectively. And the hazardous waste (CCl_4) was injected through the waste injector only. The proper locations of the injector were determined from the previous work of the main author of this paper [Chun, 1999; Chun et al., 2002].

The CCl_4 was transported with the aid of a pumpless, "blow-case" system [Bose and Senkan, 1983], consisting of a pressurized liquid reservoir tank, by high-pressure nitrogen gas, a high precision flow

[†]To whom correspondence should be addressed.
E-mail: ynchun@chosun.ac.kr

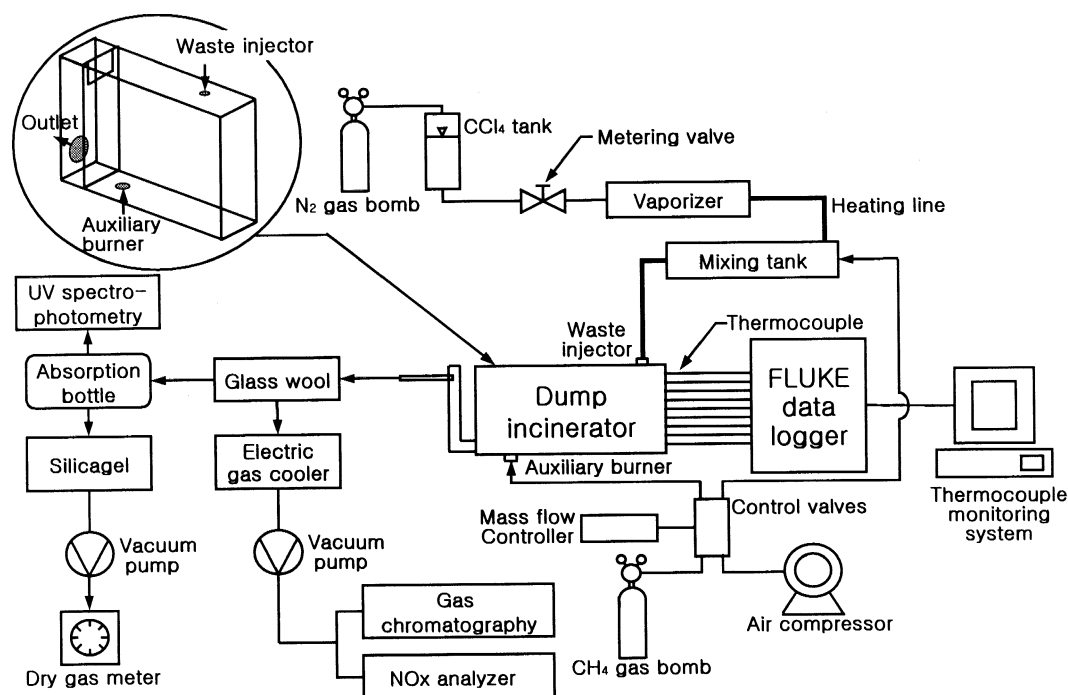


Fig. 1. The experimental setup.

regulation valve, and corresponding gauges for the monitoring of pressure and temperature. The CCl_4 was injected into the heated gas at a heating unit. All the lines, after the liquid injection, were heated to prevent condensation of the CCl_4 .

Gas sampling was achieved by the two procedures shown in Fig. 1. One was used for gas species (CH_4 , CO_2 , O_2 , CCl_4 , NO_x etc.) and the other for HCl only. The combustion gases were withdrawn from the dump incinerator by using a vacuum pump, through glass wool (to remove soot) and electric gas cooler (to condense vapor), and sampled, at time intervals, through a sampling loop in a gas chromatograph system (Shmadzu 14B). However, for the sampling of HCl, the gas was absorbed in an absorption bottle, containing sodium hydroxide.

The analysis of CH_4 , CO_2 , O_2 and N_2 gases was accomplished by using gas chromatography with Porapak Q and molecular sieve $13\times$ columns and thermal conductivity detector. Detection of waste destruction in the device was made by using DB 5 capillary columns with flame ionization detector to measure CCl_4 destruction (sensitive to 100 ppm), yielding a maximum detectable DRE of approximately 5.7 nines. NO_x and CO gases were continuously monitored by NDIR (Non-dispersive infrared) analyzer (CAI-ZRF). To measure HCl, the solvent, including this gas, was made the sample, while mercury (II) thiocyanite [$\text{Hg}(\text{SCN})_2$] and iron (III) ammonium sulfate [$\text{Fe}_2(\text{SO}_4)_3(\text{NH}_4)_2\text{SO}_4 \cdot \text{H}_2\text{O}$] were added to the solvent to giving a color. Absorptometric analysis was achieved with UV-visible spectrophotometry (U.V. Shimadzu 160A).

Temperature measurements are taken using 0.3 mm Pt/Pt-13% Rh thermocouples with Data Logger (Fluke 2625A).

MATHEMATICAL MODEL

Turbulence is modeled by using the high Reynolds version of

the two equation ($k-\epsilon$) model [Launder and Spalding, 1998]. This requires the solution of the transport equations for kinetic energy of turbulence k and its dissipation rate ϵ . In this two-equation model, the "Boussinesq" gradient hypothesis is used for the second-order velocity fluctuation correlation term and a Prandtl-Kolmogorov relationship is used to correlate the turbulent viscosity to k and ϵ .

Special attention is focused on the modeling of the turbulent reaction in a premixed CH_4 - CCl_4 -air flame. The reaction rate of this mixture is believed to be determined not only by turbulence mixing but also by chemical kinetics. This is particularly true since CCl_4 is incapable of a self-sustaining flame due to the low enthalpy of combustion and its flame inhibition. In order to resolve the non-equilibrium effects in CH_4 - CCl_4 -air flames, detailed chemical kinetic data is required. Efforts have been directed toward this end [Cundy et al., 1987; Morse et al., 1988], but, there is no well established chemical kinetic data available so far. Thus, a detailed consideration of the kinetic rates is not quite warranted at this stage. Rather, an empirical modeling approach is adopted in this study.

Fast chemistry model is applied for turbulent reaction in premixed flame, and thermal theory and the concept of burning velocity are used to describe the flame inhibition characteristics of CCl_4 which is a halogen compound.

Based on the thermal theory of flame propagation [Glassman, 1996], the reaction rate (RR) can be related to the flame burning velocity by

$$S_u \sim (\alpha \text{RR})^{1/2} \quad (1)$$

where α denotes the thermal diffusivity.

Burning velocity is available as a function of R (molar concentration ratio of CCl_4 to CH_4) and ϕ (equivalence ratio) in a laboratory Bunsen flame study [Valeiras, 1982]. Utilizing Eq. (1) and the relationship between S_u vs. R, the reaction rate expression of CH_4 -

CCl_4 -air mixture can be obtained as a function of R and ϕ as

$$\overline{\text{RR}}_{\text{CH}_4-\text{CCl}_4}|_{at R, \phi} = \frac{\left(\frac{S_u}{\alpha}\right)_{R, \phi}}{\left(\frac{S_u}{\alpha}\right)_{R=0, \phi}} \times \overline{\text{RR}}_{\text{CH}_4}|_{R=0, \phi} \quad (2)$$

In Eq. (2), $\overline{\text{RR}}_{\text{CH}_4}|_{R=0, \phi}$ described fast chemistry model only represents the reaction rate of CH_4 in a pure CH_4 -air reaction. For any value of R between experimental data points, the corresponding burning velocity S_u is obtained by linear interpolation.

The volumetric reaction rate of CH_4 ($\overline{\text{RR}}_{\text{CH}_4}$) in a CH_4 - CCl_4 -air mixture is given by the phenomenological eddy breakup model proposed by Magnussen and Hjertager [1976], i.e.,

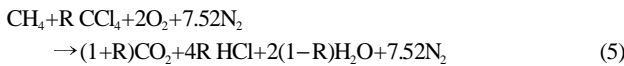
$$\overline{\text{RR}}_{\text{CH}_4} = \text{minimum of } \left[\bar{\rho} A \bar{m}_{\text{fuel}} \frac{\varepsilon}{k}, \bar{\rho} A' \frac{\bar{m}_{\text{ox}} \varepsilon}{s k}, \rho A' \frac{\bar{m}_{\text{pr}} \varepsilon}{(1+s)k} \right] \quad (3)$$

where $\bar{\rho}$ is the time-averaged density, s is the stoichiometric oxygen requirement by mass and A and A' are empirical constants given by Lockwood et al. [1980].

In order to account for the CH_4 reaction rate in CH_4 - CCl_4 -air mixture, the following expressions are used for the species mass fractions appearing in Eq. (3).

$$\begin{aligned} \bar{m}_{\text{fuel}} &= \bar{m}_{\text{CH}_4} + \bar{m}_{\text{CCl}_4} \cdot \frac{M_{\text{C}}}{M_{\text{CCl}_4}}, \quad \bar{m}_{\text{ox}} = \bar{m}_{\text{O}_2} + \bar{m}_{\text{CCl}_4} \cdot \frac{2M_{\text{Cl}_2}}{M_{\text{CCl}_4}}, \quad \text{and} \\ \bar{m}_{\text{pr}} &= \bar{m}_{\text{CO}_2} + \bar{m}_{\text{H}_2\text{O}} + \bar{m}_{\text{HCl}} \end{aligned} \quad (4)$$

Once the CH_4 reaction rate is obtained, the individual species reaction rates can be calculated by using the stoichiometric reaction expression given by Eq. (5).



In Eq. (5), as the R value increases the species mass fraction \bar{m}_{CH_4} and \bar{m}_{O_2} decreases, which results in a reduced reaction rate and finally the reaction will be quenched for large R values.

For example, CCl_4 reaction rate ($\overline{\text{RR}}_{\text{CCl}_4}$) can be expressed as

$$\overline{\text{RR}}_{\text{CCl}_4} = \overline{\text{RR}}_{\text{CH}_4-\text{CCl}_4} \times \frac{R \cdot M_{\text{CCl}_4}}{M_{\text{CH}_4} + R \cdot M_{\text{CCl}_4}} \quad (6)$$

where M denotes the molecular weight.

Further, the stoichiometric oxygen requirement(s) in Eq. (3) can be expressed as

$$s = \frac{2M_{\text{O}_2} + 2RM_{\text{Cl}_2}}{M_{\text{CH}_4} + RM_{\text{C}}} \quad (7)$$

The six flux model for radiation [Spalding, 1980] is employed for radiation heat transfer. The products of gas combustion, such as CO_2 and H_2O , are strong selective absorbers and emitters, but they do not scatter radiation significantly. The absorptivities of N_2 and O_2 are so small that these gases are almost completely transparent to radiation. Absorption and scattering coefficient are used, 1.45 m^{-1} and 0 m^{-1} , respectively. The emissivity of stainless steel, which is the material of dump incinerator, is 0.6. The contribution of radiative heat transfer to the energy equation is a source term involving the divergence of the radiative heat flux. The energy equation source term is given as Eq. (8).

$$S_{\text{rad}} = 2a[\bar{R}_x + \bar{R}_y + \bar{R}_z - 6E] \quad (8)$$

where a is absorption coefficient, E the black-body emissive power and \bar{R}_x , \bar{R}_y , \bar{R}_z composite radiation fluxes.

CALCULATIONS

The non-uniform, orthogonal computational grid with measurement points and physical dimensions is shown in Fig. 2. Inlet boundary conditions according to the flame types are listed in Table 1. Coordinate stretching has been employed to increase the grid density near the dump and heat exchanger planes because we expected

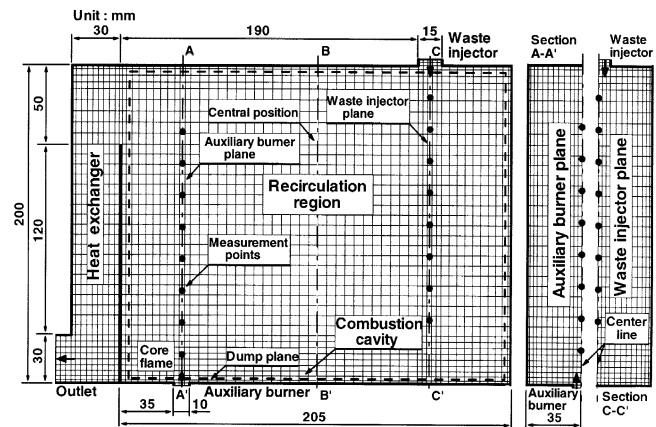


Fig. 2. Computational grid with measurement points and physical dimensions.

Table 1. Inlet boundary conditions for flame type

Flame type	Auxiliary burner				Waste injector					
	Q_{fm}	Q_{am}	ϕ_m	V_m	Q_{fw}	Q_{cw}	Q_{aw}	R	ϕ_w	V_w
Flame S	2.0	19.0	1.0	4.47	4.0	1.6	38.1	0.4	1.0	4.12
Flame 1	2.0	19.0	1.0	4.47	4.0	3.3	38.1	0.9	1.0	4.31
Flame 2	2.0	19.0	1.0	4.47	4.0	1.6	47.6	0.4	0.8	5.02

[List of symbols]

Q_f : fuel flow rate (l/min)

Q_a : air flow rate (l/min)

ϕ : equivalence ratio

Q_c : hazardous waste flow rate (l/min)

R : molar concentration ratio of CCl_4 to CH_4

V : inlet mixture velocity (m/s)

[Subscripts]

m : auxiliary burner

w : waste injector

fluid dynamic effects to be important there. Grid compaction was employed in the core flow to accurately capture the flame. The grid size was $64 \times 12 \times 40$. Calculations have been performed for the reference flame (referred to as Flame S) and were selected by computing a series of cases (See Table 1). Also, the effects of varying the molar concentration ratio of CCl_4 to CH_4 (R) (referred to as Flame 1), and the inlet velocity of the waste injector (V_w) (referred to as Flame 2), are important factors for the design and operation of the cavity incinerator, so they have been calculated.

The basic conservation equations for mass, momentum, energy, turbulence quantities, radiation flux and species concentration can be expressed, in an Eulerian Cartesian coordinate, as

$$\frac{\partial}{\partial x_i}(\rho \bar{u}_i \bar{\phi}) = \frac{\partial}{\partial x_i} \left(\Gamma_\phi \frac{\partial \bar{\phi}}{\partial x_i} \right) + S_\phi \quad (9)$$

in which ϕ denotes general dependent variables per unit mass. The dependent variables are the velocity components (\bar{u} , \bar{v} , \bar{w}), pressure (\bar{p}), turbulent kinetic energy (\bar{k}), dissipation rate ($\bar{\epsilon}$), enthalpy (\bar{h}), composite radiation flux (\bar{R}_x , \bar{R}_y , \bar{R}_z), and the mass fractions of chemical constituents (\bar{m}_{CH_4} , \bar{m}_{CCl_4} , \bar{m}_{O_2} , \bar{m}_{CO_2} , \bar{m}_{HCl} and $\bar{m}_{\text{H}_2\text{O}}$). Γ_ϕ and S_ϕ represent the turbulent diffusion coefficient and source term, respectively. Expressions for Γ_ϕ and S_ϕ are presented in Table 2, together with empirical constants for mass fractions and enthalpies of all species, where σ denotes the turbulent Prandtl/Schmidt number. In Table 2, H_{fu} is a low calorific value, given by Eq. (10).

$$H_{fu} = \frac{(8.02 + 1.73R) \times 10^8}{16 + 154R} \quad (10)$$

The Eulerian gas phase equations were solved by a control volume based finite difference procedure. A detailed description of this method is given by Patankar [1980]. In brief, the method requires the division of the computational domain into a number of control volumes, each associated with a grid point. In this study, the governing differential equations in each control volume profile are ap-

Table 2. Expressions of Γ_ϕ and S_ϕ for enthalpy and species mass fractions

ϕ	Γ_ϕ	S_ϕ
\bar{m}_{CH_4}	$\frac{\mu_{\text{eff}}}{\sigma_{\text{CH}_4}}$	$-\overline{\text{RR}}_{\text{CH}_4-\text{CCl}_4} \cdot \frac{M_{\text{CH}_4}}{M_{\text{CH}_4} + R \cdot M_{\text{CCl}_4}}$
\bar{m}_{CCl_4}	$\frac{\mu_{\text{eff}}}{\sigma_{\text{CCl}_4}}$	$-\overline{\text{RR}}_{\text{CH}_4-\text{CCl}_4} \cdot \frac{R \cdot M_{\text{CCl}_4}}{M_{\text{CH}_4} + R \cdot M_{\text{CCl}_4}}$
\bar{m}_{O_2}	$\frac{\mu_{\text{eff}}}{\sigma_{\text{O}_2}}$	$-2\overline{\text{RR}}_{\text{CH}_4-\text{CCl}_4} \cdot \frac{M_{\text{O}_2}}{M_{\text{CH}_4} + R \cdot M_{\text{CCl}_4}}$
\bar{m}_{HCl}	$\frac{\mu_{\text{eff}}}{\sigma_{\text{HCl}}}$	$4\overline{\text{RR}}_{\text{CH}_4-\text{CCl}_4} \cdot \frac{R \cdot M_{\text{HCl}}}{M_{\text{CH}_4} + R \cdot M_{\text{CCl}_4}}$
\bar{m}_{CO_2}	$\frac{\mu_{\text{eff}}}{\sigma_{\text{CO}_2}}$	$(1+R)\overline{\text{RR}}_{\text{CH}_4-\text{CCl}_4} \cdot \frac{M_{\text{CO}_2}}{M_{\text{C}_2\text{H}_6} + R \cdot M_{\text{CCl}_4}}$
$\bar{m}_{\text{H}_2\text{O}}$	$\frac{\mu_{\text{eff}}}{\sigma_{\text{H}_2\text{O}}}$	$2(1-R)\overline{\text{RR}}_{\text{CH}_4-\text{CCl}_4} \cdot \frac{M_{\text{H}_2\text{O}}}{M_{\text{CH}_4} + R \cdot M_{\text{CCl}_4}}$
\bar{h}	$\frac{\mu_{\text{eff}}}{\sigma_h}$	$\overline{\text{RR}}_{\text{CH}_4-\text{CCl}_4} \cdot H_{fu}^* - S_{\text{rad}}^{**}$

$$^*H_{fu} = \frac{(8.02 + 1.73R) \times 10^8}{16 + 154R} [\text{J/kg}]$$

Constant in combustion models

$$\sigma_{\text{CH}_4} = \sigma_{\text{O}_2} = \sigma_{\text{HCl}} = \sigma_{\text{CO}_2} = \sigma_{\text{H}_2\text{O}} = 1, \sigma_{\text{CCl}_4} = \sigma_h = 0.9$$

$^{**}S_{\text{rad}}$ is in Eq. (8)

proximated in each coordinate direction; the power-law scheme was employed for the discretization of the convection term appearing in the governing Eq. (9).

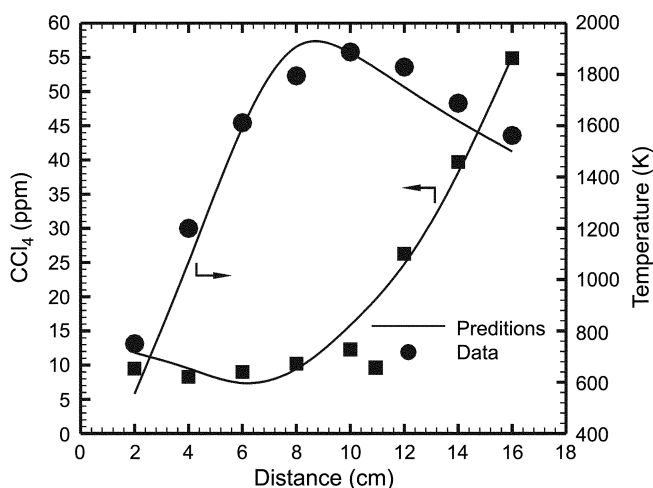
A series of discretized linear equations were solved iteratively due to the nonlinear feature of the equation implicitly imbedded in the coefficient of the discretized equation. The composite radiation fluxes in RTEs (radiative transfer equations) were solved in relation to the conduction term (i.e., first term) in Eq. (9) omitted. The fluid must only convect the residence time, so that the diffusion term is deactivated. The SIMPLEST (Semi-Implicit Method for Pressure-Linked equations Shortened) algorithm, a derivative SIMPLE, was used for the differential equation numerical procedures [Spalding, 1988], to enclosure rapid convergence.

RESULTS AND DISCUSSIONS

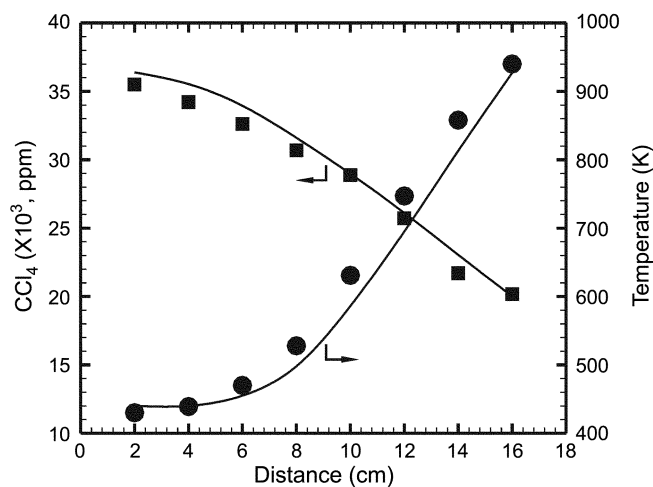
1. Comparison of Predictions and Measurements

Predictions of a dump incinerator include flow-velocity distribution, gas temperature and concentrations of major species (CH_4 , CCl_4 , O_2 , CO_2 , HCl etc.).

Detailed comparisons have been made, between the selected model predictions and dump incinerator-probing measurements, on a



(a) Auxiliary burner plane



(b) Waste injector plane

Fig. 3. Comparison between predictions and experimental data.

dry basis for Flame S.

Fig. 3 shows selected gas concentrations and temperature at the centerline of the auxiliary burner plane and of the waste injector plane, respectively. The points are the experimental data in all the figures. The overall agreement between predictions and experimental data were found to be good, as shown in the figures. Considering the complexity of that which is being modeled, the agreement between the predictions and data is on the whole a pertinent approach.

In order to resolve the non-equilibrium effects in CH₄-CCl₄-air flames, an empirical modeling approach was adopted in this study. However, the flame burning velocity, $S_{u,s}$ in Eq. (2), used a fully developed laminar flame from the laboratory Bunsen burner [Valeiras, 1982], owing to a lack of available data for turbulent flames. If the detailed data of flame burning velocity, which is considered a turbulent effect, had been used for the calculation of reaction rate in Eq. (6), more reasonable predictions may have been achieved.

2. CFD Analysis

2-1. Cavity Hydrodynamics and Flame Structure

The cavity hydrodynamics, and flame structure, in a cavity incinerator were studied with Flame S, as being good operating conditions, as selected by computing a series of cases. The inlet stream conditions of Flame S are a molar concentration ratio of CCl₄ to CH₄ (R) with an inlet velocity at the waste injector (V_w) of 0.4 and 4 m/s, respectively.

Selected results at the center plane, auxiliary burner and waste injector plane (refer to Fig. 2) are presented in Figs. 4-6.

Velocity vector fields are shown in Fig. 4. When the mixture is introduced at the auxiliary burner, a large recirculation region is formed within the combustion cavity by the rearward facing step. The formation of this recirculation region is important for a long residence time, at high temperature, for the destruction of hazardous waste. A recirculation zone is built up at the right of rearward facing step, by inflowing waste at the waste injector. This may aid the flame at the waste injector to burn more stably, by giving latent heat to the inflowing waste mixture.

The cavity hydrodynamics are related to the incinerator configuration and aspect ratios [Chun, 1999; Chun et al., 2002]. Further, the inflowing mixture conditions at the auxiliary burner, and the location of the waste injector, in the combustion cavity, have a very significant impact on the structure of the recirculation region, in

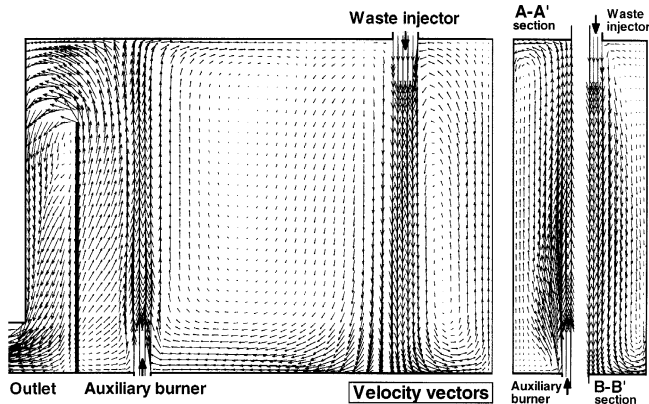


Fig. 4. Calculated velocity vector fields.

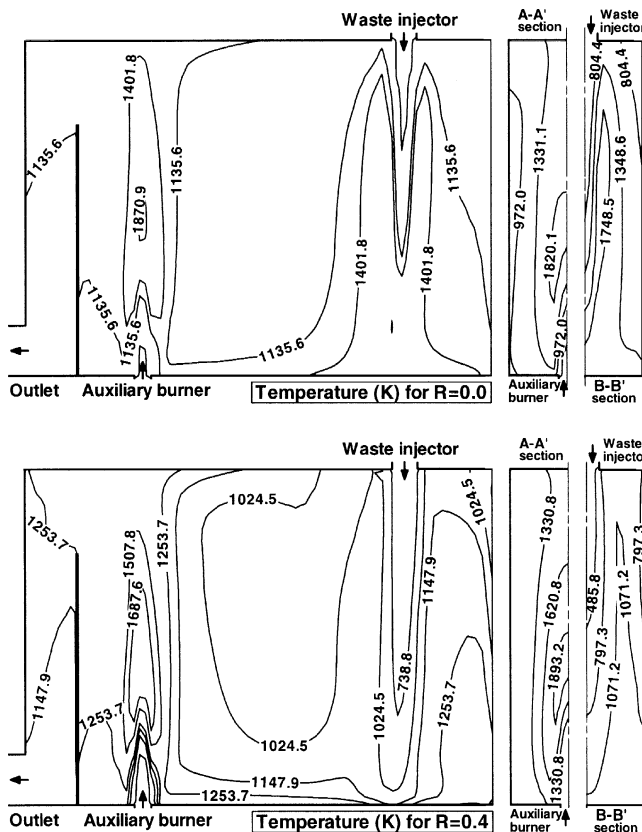


Fig. 5. Temperature field contours for R=0.0 and R=0.4.

some cases completely changing the nature of the flow within the cavity.

Fig. 5 presents the temperature field contours for R=0.4 (i.e., Flame S) and R=0.0 (i.e., pure CH₄ flame) to see the inhibiting effect of CCl₄.

In the case of R=0, where CCl₄ is not introduced as a surrogate at the waste injector, both the flames of auxiliary burner, and waste injector, burned stably with higher temperatures than when R=0.4, particularly at the waste injector.

However, for Flame S when R=0.4, a lift flame with a lower temperature was formed at the waste injector due to the inhibiting effect of CCl₄. Therefore, most of the waste mixture burns in the recirculation region. The inhibiting effect of halogens on the oxidation of hydrocarbon/air flames has been studied and defined by Westbrook and Dryer [Westbrook and Dryer, 1981], who suggested the inhibitor provides competition for radical species, particularly H atoms. Regardless of the inhibiting effect at the waste injector, the flame of the auxiliary burner burns stably. It could maintain higher temperatures in the recirculation region, and the heat exchanger, being particularly effective for the destruction of hazardous wastes. High temperature in heat exchanger contributes to the complete destruction of CCl₄ that could not be destroyed in the recirculation region.

As a result, the cavity incinerator designed in this study may guarantee complete destruction, because most of the wastes burn in the recirculation region, and complete burning is possible at the heat exchanger.

Fig. 6 presents selected gas concentrations in a cavity incinerator.

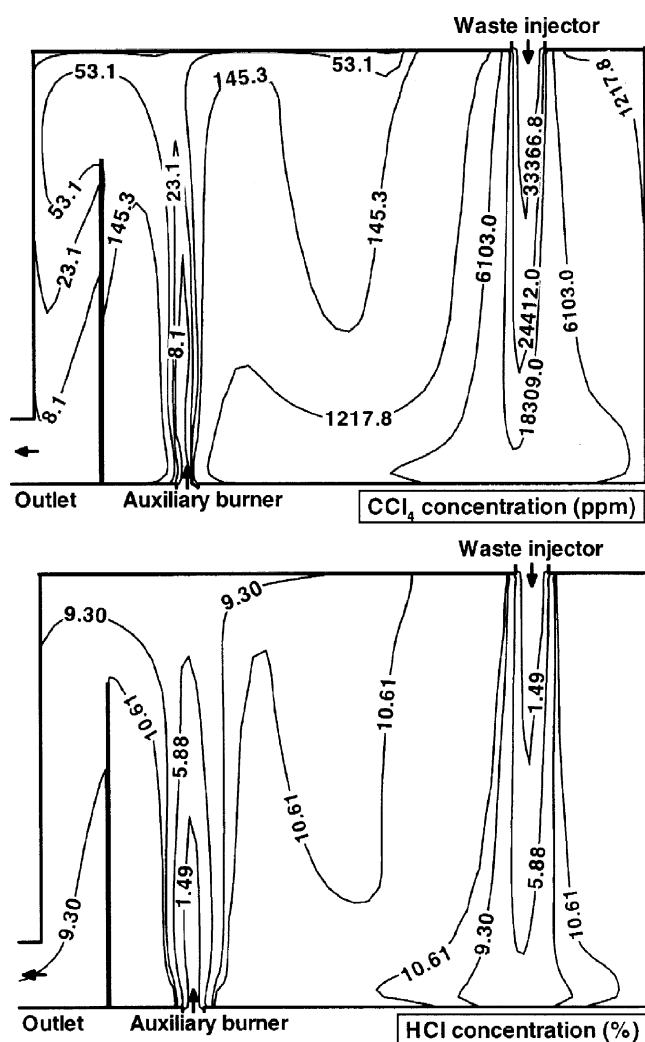


Fig. 6. Selected gas concentrations.

The CCl_4 decreases drastically toward the flame-front, while CCl_4 inflowing from the waste injector decreases gradually within the core-shape mixture flow. Remaining CCl_4 is completely destroyed through the recirculation region and heat exchanger. DRE yielded from CCl_4 concentration is 99.99% at the outlet. CCl_4 destruction of 99.99% is of the same orders required by the EPA of 99.99% ("4 nines") DRE for hazardous waste incinerators [Oppelt, 1987].

Most of the HCl is produced at the long flame-front in the core-type flow of the waste injector, due to the destruction of the inflowing CCl_4 waste at the injector only. The lower concentrations at the auxiliary burner and heat exchanger stream are because the species produced at the flame-front of the auxiliary burner and recirculation region are diluted.

2-2. Effect of Varying the Parameters

Parametric studies were made in order to resolve the effects of the molar concentration ratio of CCl_4 to CH_4 (R), and the inlet velocity at the waste injector (V_w). For Flame 1, R was increased to 0.9, and for Flame 2, V_w was increased to 5 m/s.

Figs. 7 and 8 show selected predictions along a centerline of the waste injector plane for Flames 1 and 2, respectively.

The selected predictions for Flame 1, with R changed to 0.9, are

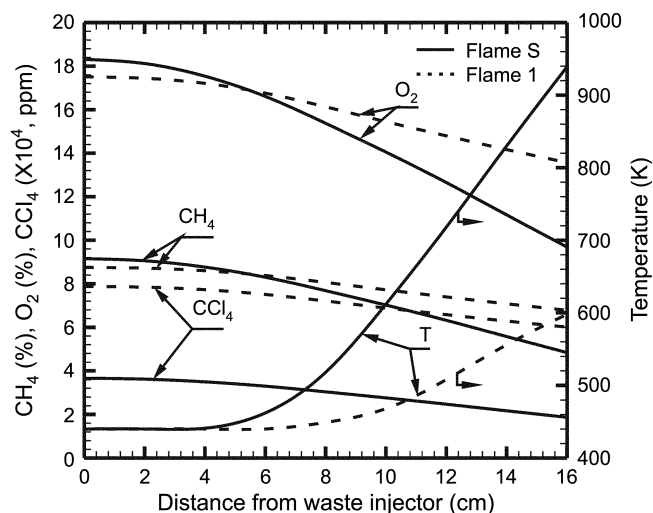


Fig. 7. Selected predictions for Flame 1, with R changed to 0.9.

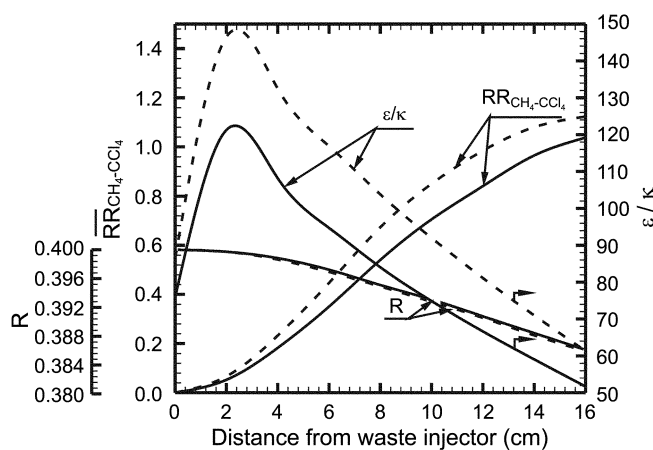
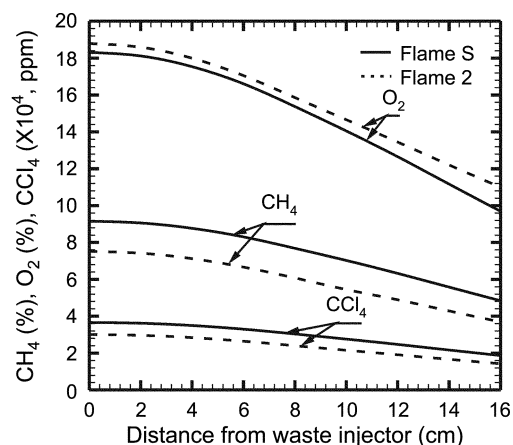


Fig. 8. Selected predictions for Flame 2, with V_w changed to 5 m/s.

shown in Fig. 7, and indicate the effect of the molar concentration ratio of CCl_4 to CH_4 .

The concentrations of CH_4 and O_2 near the waste injector are lower when $R=0.9$ due to inflow having a lower mole fraction. This trend is reversed due to the much greater inhibition of the species destruction. Therefore, the temperature is significantly depressed, showing much higher CCl_4 concentration. This gives a DRE at the

outlet of 95.98%, which is much lower than EPA requirement [Oppelt, 1987].

We can see that the choice of an operational parameter, such as chlorine to hydrogen loading (CCl_4/CH_4), at the waste injector is an important factor in CCl_4 destruction in a cavity incinerator.

Selected predictions for Flame 2 with V_w changed to 5.02 m/s, as shown in Fig. 8, to see the effect of the inlet stream velocity.

The destructions of CH_4 and CCl_4 were higher than in Flame S. This was due to higher turbulent mixing due to the increased inlet stream velocity. As mentioned earlier, the reaction rate for the case of slow chemistry is believed to be determined, not only by turbulence mixing, but also by the chemical kinetics. For Flame 2, the R value at the waste injector, which plays a part in flame inhibition, is unchanged. Therefore, the reaction rate for this flame has most effect on the turbulent mixing, although the R value calculated in the cavity incinerator is slightly decreased by greater combustion. Turbulent mixing may be represented by the inverse of eddy break-up time, ϵ/k as in Eq. (1). As the Reynolds number (i.e., inlet stream velocity) increases, the turbulence scale, from isotropic turbulence theory, is expected to decrease. A turbulent flow at a relatively high Reynolds number has a relatively fine, small-scale, structure compared to a turbulent flow at a lower Reynolds number, but with the same integral size. Therefore, as inlet stream velocity increases, the reaction rate (i.e., $\overline{\text{RR}}_{\text{CH}_4-\text{CCl}_4}$) in Eq. (1), which is proportional to ϵ/k , is expected to increase. As a result, the DRE of 99.9992% at the outlet is thus five orders of magnitude above the EPA requirement [Oppelt, 1987].

In spite of greater combustion, a higher O_2 concentration remains due to the excess air introduced at the waste injector, by decreasing the equivalence ratio to 0.8. Generally, the conventional incineration strategy introduces excess air to ensure complete combustion of the waste stream. However, we can see that it is not a good application to the incineration of CHC's because of the following Deacon reaction [Jones et al., 1966].



Excess oxygen can lead to pure chlorine gas, which is more difficult to scrub out of stack gases than HCl.

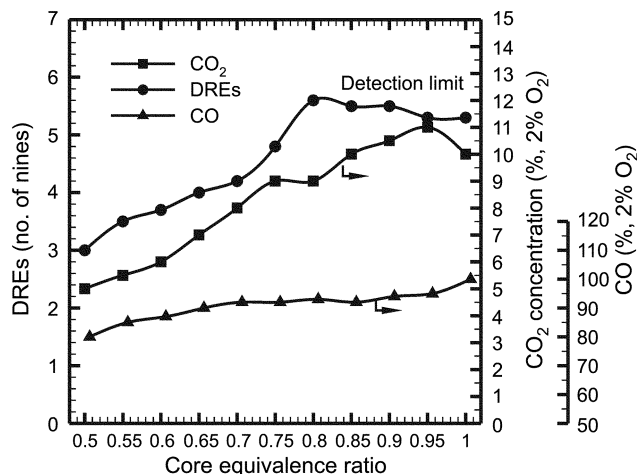
3. Experimental Test

Experiments were conducted to show the attainment of desired DRE, before the application to a full-scale plant. All data in Figs. 9 and 10 are mean values measured through replicate experiments.

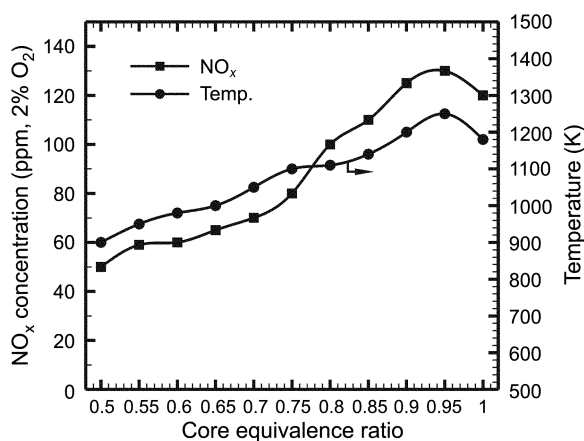
Fig. 9 shows species concentrations, DREs, and temperatures, according to the variation of core equivalence ratio of the auxiliary burner. The equivalence ratio at the waste injector and the molar concentration ratio of CCl_4 to CH_4 were both 1.0.

As one would expect, the concentration of CO_2 increased with the increase in core equivalence ratio (accomplished here by increasing the auxiliary fuel flow rate), while the CO concentration was almost unchanged with excess air. The maximum value of CO_2 was shown at a core equivalence ratio of 0.95, as shown in Fig. 9(a).

The DRE profiles were expected to show a similar pattern to that of CO_2 , indicating good combustion. The highest destruction was shown as 5.6 nines, with a core equivalence ratio of 0.8. This may be the detection limit of the GC for CCl_4 . Therefore, it is quite possible that higher destruction was achieved with a core air ratio of



(a) DREs and selected species concentration



(b) NO_x and gas temperature

Fig. 9. DREs, selected species measurements and temperature as a function of core equivalence ratio at auxiliary burner.

0.95, which showed the maximum concentration of CO_2 . With closer stoichiometry, the primary reaction at the cavity plane produces a hotter reaction, resulting in an increase in the rate of destruction of CCl_4 in the recirculation region. Further, even though the highest destruction was shown in conditions with excess air, DRE at which the core equivalence ratio was 1.0 (in the case that the total equivalence ratio was 1.0), was five orders of magnitude greater. This means our cavity incinerator with closer stoichiometry could achieve destruction above the EPA requirement of 99.99% ("4 nines") DRE for hazardous waste incinerators [Oppelt, 1987], in which no pure chlorine gas is produced by the Deacon reaction [Jones et al., 1966].

However, thermal NO_x , which is produced at higher temperatures, as shown in Fig. 9(b), increased with the increase in the CCl_4 destruction rate. These observations suggest thermal NO_x must be controlled by other technology, for example, an external oscillation [Cole et al., 2001] for low emission control.

Fig. 10 shows DREs, species concentrations and temperatures, according to the variation of the molar concentration ratio of CCl_4 to CH_4 . The core equivalence ratio for the auxiliary burner and waste injector were both 1.0.

DREs, NO_x and temperature decreased with the increase in the molar concentration ratio of CCl_4 to CH_4 , while CO concentrations

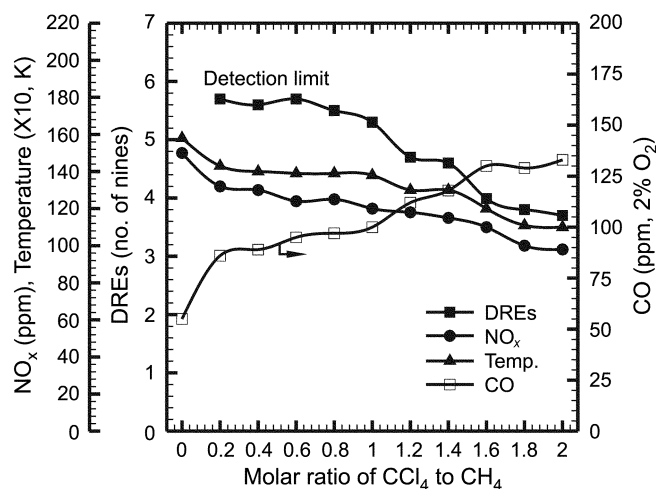


Fig. 10. DREs, species measurements and temperature as a function of molar concentration ratio of CCl₄ to CH₄.

increased. The decrease of DREs and NO_x was because the lower temperature caused by heat release in the recirculation region due to pyrolysis of CCl₄. The increase of CO is due to the increase of carbon, which increased the molar concentration ratio of CCl₄ to CH₄. When the molar ratio of CCl₄ to CH₄ is more than 1.6, DRE failed, and were three orders of magnitude below the EPA requirement [Oppelt, 1987]. This was due to the temperature being below 1,000 °C in the recirculation region.

SUMMARY AND CONCLUSIONS

In order to obtain a more reliable predictive procedure for a cavity incinerator design and operating conditions, complex 3-dimensional flow field calculations were achieved, and validated by comparison to experimental data, as shown in Fig. 3. The overall agreement between the predictions and experimental data were found to be good. Results indicate that CCl₄ has a strong quenching effect on the chemical reaction, due to the flame inhibition feature of halogen compounds and the associated kinetic effects must be incorporated, as the empirical model in this study, in order to obtain realistic predictions.

Cavity dynamics and flame structure were studied on a flame selected by computing a series of cases in the complex hydrodynamic environment of the cavity incinerator designed for this study. For the good destruction of hazardous waste, it was effective when the waste was injected into the recirculation region with high temperature, when the conditions did not disturb the combustion cavity. The core flame in the auxiliary burner had a significant impact on the structure of the recirculation region, in some cases completely changing the nature of the flow within the cavity.

The parametric studies were made in order to resolve the effects of the molar concentration ratio of CCl₄ to CH₄ and the inlet stream velocity at the waste injector. The molar concentration ratio of CCl₄ to CH₄ was an important factor for the destruction of CCl₄. Greater CCl₄ destruction was shown as the inlet stream velocity was increased. Although DRE was somewhat increased by a lower equivalence ratio at the waste injector, it was reasonable to select an equivalence ratio (ϕ_w) of 1. This was because excess oxygen, which can lead to

pure chlorine gas, is more difficult to scrub out of stack gases than HCl.

The DREs in our 5.2 kW laboratory scale cavity incinerator were five orders of magnitude above the EPA requirement of 99.99% ("4 nines") DRE for hazardous waste incinerators [Oppelt, 1987]. However, thermal NO_x produced at high temperatures, increases with the increase in CCl₄ destruction rate. To achieve low emission combustion in a cavity incinerator, thermal NO_x must be controlled with other technology, for example, an external oscillation [Cole et al., 2001].

REFERENCES

- Bose, D. and Senkan, S. M., "On the Combustion of Chlorinated Hydrocarbons: I. Trichloroethylene," *Comb. Sci. and Tech.*, **35**, 187 (1983).
- Chun, Y. N., Lee, K. J. and Song, H. O., "Numerical Simulation of Hazardous Waste Destruction in Three-dimensional Dump Incinerator," *Korean J. Chem. Eng.*, **19**, 20 (2002).
- Chun, Y. N., "Numerical Simulation of Dump Combustor with Auxiliary Fuel Injection," *J. of KSME*, **13**, 948 (1999).
- Cole, J. A., Widmer, N. C., Seeker, W. R., Schadow, K. C., Parr, T. P. and Wilson, K. J., "Research and Development to Improve Naval Shipboard Waste Management Using a Compact Closed Loop Controlled Waste Incinerator," *Chemosphere*, **42**, 765 (2001).
- Cundy, V. A., Morse, J. S., Lester, T. W. and Senser, D. W., "An Investigation of a Near-stoichiometric CH₄/CCl₄/Air Premixed Flat Flame," *Chemosphere*, **6**, 989 (1987).
- Glassman, I., "Combustion," Academic Press, New York, 118 (1996).
- Gutmark, E. J., Parr, T. P., Wilson, K. J., Yu, K. H., Smith, R. A., Hanson-Parr, D. M. and Schadow, K. C., "Compact Waste Incinerator Based on Vortex Combustion," *Combust. Sci. and Tech.*, **121**, 333 (1996).
- Jones, A., Bliss, H. and Walker, C., "Rates of Hydrogen Chloride Oxidation," *AICHE J.*, **12**, 260 (1966).
- Lauder, B. W. and Spalding, D. B., "Mathematical Models of Turbulence," Academic Press, New York (1998).
- Liou, T. M., Lee, H. L. and Liao, C. C., "Effects of Inlet Guide-vane Number on Flowfields in a Side-dump Combustor," *Experimental Thermal and Fluid Science*, **24**, 11 (2001).
- Lockwood, F. C., Salooja, A. P. and Syed, S. A., "A Prediction Method for Coal-furnaces," *Combustion and Flame*, **38**, 1 (1980).
- Magnussen, B. F. and Hjertager, H., "On Mathematical Modeling of Turbulent Combustion with Special Emphasis on Soot Formation and Combustion," 16th Symposium (International) on Combustion, The Combustion Institute, Pittsburgh, PA, 714 (1976).
- McKenty, F., Gravel, L. and Camarero, R., "Numerical Simulation of Industrial Boiler," *Korean J. Chem. Eng.*, **16**, 4 (1999).
- Morse, J. S., Cundy, V. A. and Lester, T. W., "Thermal Destruction of Carbon Tetrachloride," 1988 Spring Meeting, Western section, March 21-22, Salt Lake City, Utah, the Combustion Institute, 299 (1988).
- Oppelt, T., "Incineration of Hazardous Waste: A Critical Review," *J. Air Pollut. Control Assoc.*, **37**, 558 (1987).
- Patankar, S. V., "Numerical Heat Transfer and Fluid Flows," Hemisphere, Washington, D.C. (1980).
- Spalding, D. B., "PHOENICS Training Course Notes," CHAM TR/300 (1988).

- Spalding, D. S., "Idealizations of Radiation, In Mathematical Modeling of Fluid-mechanics," Heat Transfer and Chemical-reaction Process, Lecture 9, HTS/80/1, Imperial College, Mech. Eng., Dept., London (1980).
- Stone, C. and Menon, S., "Numerical Simulation of Combustion Dynamics in a Swirling Flow Dump Combustor," High Performance Computing 2001, Grand Challenges in Computer Simulations, April 22, Seattle, WA (2001).
- Valeiras, H. A., "Burning Velocities and Rates of Methane-chlorinated Hydrocarbon Flame," M.S. Thesis, Massachusetts Institute of Technology, Chemical Engineering (1982).
- Westbrook, C. K. and Dryer, F. L., "Inhibition Effect of Halogens on the Oxidation of Hydrocarbon/air Flames," 18th Symposium (International) on Combustion, The Combustion Institute, Pittsburgh, 749 (1981).